

## Role of $Mn^{2+}$ and $Mg^{2+}$ in Catalysis and Regulation of *Aspergillus niger* Glutamine Synthetase

N S PUNEKAR\*, C S VAIDYANATHAN & N APPAJI RAO

Department of Biochemistry, Indian Institute of Science, Bangalore 560012

Received 3 December 1984, revised 15 April 1985

The kinetic data on the effect of  $Mn^{2+}$ ,  $Mg^{2+}$ , and ATP on the *Aspergillus niger* glutamine synthetase activity analysed according to the isovelocitv method [London W P & Steck T L (1969) *Biochemistry*, **8**, 1767] revealed that the enzyme under physiological conditions is probably an Mn(II) enzyme. Excess of ATP or  $Mn^{2+}$  beyond the concentrations required to form the metal ion-nucleotide complex inhibited both the  $Mg^{2+}$  and  $Mn^{2+}$  supported glutamine synthetase activity, whereas excess  $Mg^{2+}$  was not inhibitory. These results along with the inhibition of enzyme activity by  $Ca^{2+}$ ,  $Zn^{2+}$ ,  $Co^{3+}$ , GTP and EDTA indicated that the interactions of the enzyme with  $Mn^{2+}$  and  $Mg^{2+}$  were different. Supporting evidence for the proposed kinetic mechanism was obtained by the protection afforded by low concentrations of  $Mn^{2+}$  (<100  $\mu M$ ) against inactivation of the enzyme by *N*-ethylmaleimide or phenylglyoxal. However, ATP enhanced the rates of inactivation by both modifying agents.  $K_{Mn^{2+}}$  values of 52 and 14  $\mu M$  calculated from the protection afforded by this metal ion against inactivation by phenylglyoxal and *N*-ethylmaleimide suggested the presence of a high affinity  $Mn^{2+}$  binding site on the enzyme, in addition to the binding of  $Mn^{2+}$ -ATP complex at the active site. These results permit the conclusion that *A. niger* glutamine synthetase may be an Mn(II) dependent enzyme under physiological conditions and the metal ion in addition to serving as a substrate when complexed with ATP may have an additional role in protecting the enzyme against inactivation.

Glutamine synthetase (L-glutamate: ammonia ligase, EC 6.3.1.2) catalyzes the formation of glutamine, a precursor for the synthesis of a variety of nitrogenous end products. The activity and content of this enzyme located at a crucial point in the highly branched pathway of nitrogen metabolism, is regulated particularly in microorganisms by alterations in the growth medium, by accumulated end products and by availability and nature of divalent metal ion activator<sup>1-4</sup>. A derangement of carbohydrate metabolism leading to excretion of citric acid into the medium by *Aspergillus niger* is extensively used for the production of this compound by fermentation. The conditions of fermentation, viz. low pH, high amounts of carbon source and essentially  $Mn^{2+}$ -deficient medium<sup>3</sup>, resulting in elevated intracellular  $NH_4^+$  pools<sup>5</sup>, accumulation of L-glutamate, L-glutamine and amino acids derived from it<sup>7</sup> suggested to us that the metabolic interlock between carbon and nitrogen metabolism may have been deranged at the glutamine synthetase step. Although at first glance the increase in glutamine levels<sup>6,7</sup> appears to be not in agreement with the above hypothesis, a closer examination of their data, especially when ratios of L-glutamate or L-

glutamine vs time and the amounts of amino acids derived from glutamate are plotted, reveals that the decrease in glutamine synthetase flux becomes significant during citric acid fermentation. Our earlier work revealed that the activity of glutamine synthetase from *A. niger* was not regulated by covalent modification, specific proteolytic inactivation or by effective feedback inhibition<sup>8,9</sup>. However, as citric acid excretion occurred when the concentration of  $Mn^{2+}$  in the medium was very low and as one of the biosynthetic activities of glutamine synthetase required manganese ions, it was of interest to examine the role of  $Mn^{2+}$  and  $Mg^{2+}$  ions in the catalysis and regulation of the homogeneous glutamine synthetase isolated from *A. niger*<sup>9</sup>. This paper describes kinetic analysis to indicate the possible presence of a tight binding site for  $Mn^{2+}$  and a relatively weak metal ion binding site on the enzyme where  $Mn^{2+}$  or  $Mg^{2+}$  nucleotide complexes can bind as substrates.

### Experimental Procedures

Reagents including ATP, sodium L-glutamate, hydroxylamine hydrochloride, GTP, imidazole, phenylglyoxal and *N*-ethylmaleimide (NEM) were purchased from Sigma Chemical Company, St. Louis, Missouri, USA. All other reagents were of the analytical grade. ATP, GTP and EDTA were neutralized to pH 7.0 with 2 M NaOH.

**Enzyme assays**—Glutamine synthetase from *A. niger* was purified to homogeneity, as determined by polyacrylamide gel electrophoresis (PAGE) and sodium dodecyl sulphate (SDS) - PAGE, by

\*Present Address: Institute for Enzyme Research, 1710, University Avenue, MADISON, Wisconsin 53705, USA

**Abbreviations used:** NEM, *N*-ethylmaleimide; DEAE-, diethylaminoethyl-;  $K$ , dissociation constants from either kinetic or protection experiments;  $k$ , inactivator rate constant;  $\gamma$ -GHA,  $\gamma$ -glutamyl-hydroxamate; *E*, free enzyme; *M*, metal ion ( $Mn^{2+}$  or  $Mg^{2+}$ ); PAGE, polyacrylamide gel electrophoresis; SDS, sodium dodecyl sulphate.

ammonium sulphate fractionation, diethylaminoethyl (DEAE) - sephacel chromatography, AMP-sepharose affinity chromatography and gel filtration on Sepharose 4B<sup>8,9</sup>.

Glutamine synthetase activity was determined by estimating  $\gamma$ -glutamylhydroxamate ( $\gamma$ -GHA) as described elsewhere<sup>9,10</sup>.

Protein was estimated according to the method of Lowry *et al.*<sup>11</sup>, using bovine serum albumin as the standard.

One unit of enzyme activity is defined as the amount of enzyme required to produce one  $\mu$ mole of  $\gamma$ -GHA per min at 28°C.

**Chemical modifications**—*A. niger* glutamine synthetase was inactivated completely on incubating with phenylglyoxal or NEM<sup>9</sup>. For monitoring the inactivation of the enzyme by NEM, it was passed through a G-25 column (1 × 5 cm) just before use to remove 2-mercaptoethanol added to stabilize the enzyme. The inactivation of the enzyme by either phenylglyoxal (10 mM) or NEM (0.4 mM) was carried out at 28°C by incubating the enzyme (40-60  $\mu$ g) in a scaled up reaction mixture (500  $\mu$ l) and with drawing aliquots (50  $\mu$ l) at different time intervals indicated in the legends to the figures. The reaction was terminated by diluting the enzyme directly into assay mixtures which did not contain the inactivating agent. It was ensured that the chemical modification reaction was not occurring during the time required for estimating the enzyme activity. The velocity of the enzyme catalyzed reaction at zero time, i.e. immediately after the addition of inactivating agent, was normalized to 100 and the residual activity after different periods of inactivation was expressed as per cent of this normalized value. There was a parallel loss of both Mg<sup>2+</sup> dependent synthetase and Mn<sup>2+</sup> dependent transferase activity, when the enzyme was inactivated by these reagents. Similarly, the protection afforded by the various ligands against inactivation of the enzyme by the two reagents was identical for both the enzyme activities and was monitored by including the compounds in the inactivating system at appropriate concentrations. Hence  $\gamma$ -glutamyl-transferase activity values alone are reported to represent inactivation data. Phenylglyoxal interfered with the colorimetric assay<sup>10</sup> and appropriate controls were run to circumvent this problem.

Binding constants were estimated by the ability of Mn<sup>2+</sup> or Mg<sup>2+</sup>-ATP complex to protect the enzyme against inactivation by NEM or phenylglyoxal<sup>12,13</sup> using the following equation:

$$\ln \frac{k_o - k_p}{k_p} = n \ln [P] - \ln K_p \quad \dots (1)$$

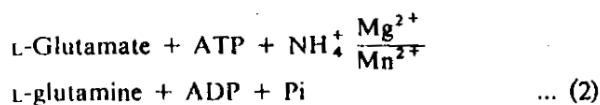
where  $k_o$  represents the rate constant of inactivation in the absence of protective ligand P,  $k_p$ , the rate constant of inactivation in the presence of ligand P and [P], the molar concentration of the ligand. A plot of  $\ln[(k_o - k_p)/k_p]$  against  $\ln[P]$  yields a straight line whose slope indicates the number of molecules of P bound per active site and the ordinate intercept ( $-\ln K_p$ ) provides the dissociation constant,  $K_p$  for the E-P complex.

**Analysis of data**—The isovelocity method and other analytical replots suggested by London and Steck<sup>14</sup> were employed to analyze the activity profiles of both Mn<sup>2+</sup> and Mg<sup>2+</sup> supported glutamine synthetase activity.

The kinetic data were analyzed by least-square curve fitting procedures (linear regression) using a programmable pocket calculator (Texas Instruments SR-51A).

## Results

**Interaction of *A. niger* glutamine synthetase with divalent cations**—The biosynthetic reaction (Eq.2) of *A. niger* glutamine synthetase required either Mg<sup>2+</sup> or Mn<sup>2+</sup> as metal ion activator



and ATP as the nucleotide substrate. Several divalent metal ions such as Ca<sup>2+</sup>, Ba<sup>2+</sup>, Sr<sup>2+</sup>, Zn<sup>2+</sup>, Cu<sup>2+</sup>, Fe<sup>2+</sup>, Co<sup>2+</sup> and Cr<sup>2+</sup> could not replace either Mg<sup>2+</sup> or Mn<sup>2+</sup> (ref.9), although many of these complex with ATP<sup>9</sup>. The study of the effect of GTP, EDTA and divalent metal ions on the Mn<sup>2+</sup>-dependent synthetase activity showed that while excess Mn<sup>2+</sup> inhibited the enzyme activity, excess Mg<sup>2+</sup> was without any effect (Table I). Also, Ca<sup>2+</sup> and Zn<sup>2+</sup> inhibited the enzyme reaction at all concentrations of Mn<sup>2+</sup> studied. Cobalt (II), however, was without any effect at the optimal Mn<sup>2+</sup> concentration but caused a very significant activation at a low concentration of Mn<sup>2+</sup> (1 mM) and less marked activation at excess Mn<sup>2+</sup> (10 mM). GTP inhibited the enzyme activity at 1 and 4 mM Mn<sup>2+</sup> and at 5 and 10 mM Mg<sup>2+</sup>. Although the effect of EDTA was qualitatively similar to that of GTP, it was quantitatively more pronounced.

The concentration of Mg<sup>2+</sup> beyond 20 mM had no significant effect on the Mg<sup>2+</sup> dependent synthetase activity (Fig 1A and Table I). Ca<sup>2+</sup> and Zn<sup>2+</sup> very specifically inhibited the Mg<sup>2+</sup> supported biosynthetic reaction at all concentrations of Mg<sup>2+</sup>. Cobalt, on the other hand, enhanced the activity at the lowest concentration of Mg<sup>2+</sup> (5 mM), and was without effect at higher concentrations of Mg<sup>2+</sup>. It is interesting to note that Co<sup>2+</sup>, Zn<sup>2+</sup> and Cd<sup>2+</sup> do not substitute for

Table 1—Effect of GTP, EDTA and Divalent Metal Ions, on the *A. niger* Glutamine Synthetase Activity

Addition (mM)	Activity (%) <sup>a</sup>					
	Mn <sup>2+</sup> (mM)			Mg <sup>2+</sup> (mM)		
	1	4	10	5	10	20
None	18	100 <sup>b</sup>	45	6	95	100 <sup>c</sup>
+Ca <sup>2+</sup> (10)	9	24	29	0	1	3
+Zn <sup>2+</sup> (10)	8	11	12	1	2	1
+Co <sup>2+</sup> (10)	107	102	77	67	90	82
+GTP (5)	4	62	71	2	47	92
+EDTA (5)	0	6	101	0	76	105

<sup>a</sup>The reaction mixtures contained 100 mM imidazole hydrochloride buffer pH 7.8 for Mg<sup>2+</sup>-dependent synthetase activity and pH 5.5 for Mn<sup>2+</sup>-dependent synthetase activity, 50 mM NH<sub>2</sub>OH, 100 mM L-glutamate, 10 mM ATP and various additions at concentrations shown in the table. The reaction was started by the addition of enzyme.

<sup>b</sup>The Mn<sup>2+</sup>-dependent synthetase activity (pH 5.5) at optimal concentration of Mn<sup>2+</sup> (4 mM) was normalized to 100 and the other numbers are per cent of this normalized value.

<sup>c</sup>The Mg<sup>2+</sup>-dependent synthetase activity (pH 7.8) at optimal concentration of Mg<sup>2+</sup> (20 mM) was normalized to 100 and the other values are expressed as per cent of this activity.

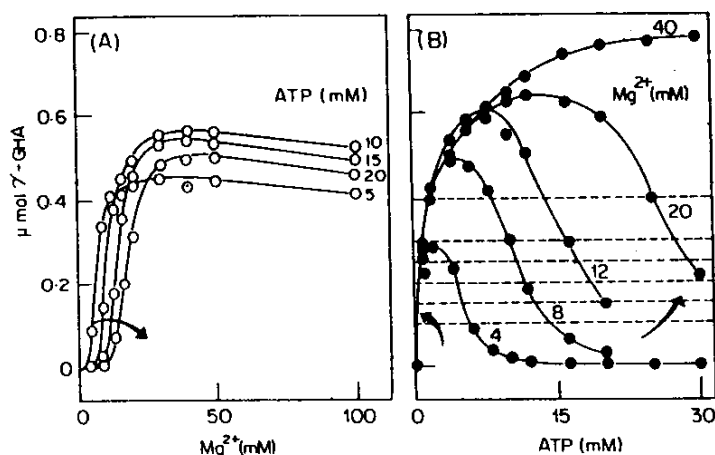


Fig. 1—Saturation of *A. niger* Mg<sup>2+</sup>-dependent glutamine synthetase activity by Mg<sup>2+</sup> and ATP [(A), Mg<sup>2+</sup>-profiles. The reaction mixture (0.5 ml) contained 100 mM imidazole hydrochloride buffer (pH 7.8), 50 mM NH<sub>2</sub>OH and 100 mM L-glutamate. MgCl<sub>2</sub> concentration was varied in the range 0–10 mM at 5, 10, 15 and 20 mM ATP. The reaction was started by the addition of enzyme (9.6 μg). (B), ATP-profiles. The enzyme assays were carried out in the same manner as described above with ATP concentration varied in the range 0–30 mM at 4, 8, 12, 20 and 40 mM MgCl<sub>2</sub>. Broken horizontal lines indicate the isovelocitivity points used for the replots in Fig. 2B. Arrows indicate the change in sigmoidicity with increasing fixed concentrations of the ligand].

Mn<sup>2+</sup> or Mg<sup>2+</sup> as metal activators. It is also clear from Table 1 that GTP inhibited the activity at 5 and 10 mM Mg<sup>2+</sup>. The effect of EDTA was similar to that observed with GTP.

Increasing concentrations of Mn<sup>2+</sup> ions progressively inhibited the Mg<sup>2+</sup>-supported glutamine synthetase reaction, with 0.2 mM Mn<sup>2+</sup> causing 50% inhibition. In view of these differences and complexity in the pattern of interaction of glutamine synthetase with Mg<sup>2+</sup> and Mn<sup>2+</sup>, the effect of these metal ions was examined in more detail.

In several experiments, the enzyme was preincubated with either the divalent metal ion (Mg<sup>2+</sup> or

Mn<sup>2+</sup>) or the nucleotide (ATP) before starting the reaction by the addition of one of the substrates. Also, in the case of *E. coli* glutamine synthetase, Mn<sup>2+</sup> converts the enzyme into a "taut" form and a lag in the time course of the synthetase reaction is observed<sup>16</sup>. It was therefore necessary to establish that preincubation of *A. niger* enzyme with these ligands did not cause either a lag or burst in the initial velocity of the reaction. When the glutamine synthetase reaction was started by the addition of enzyme, ATP, NH<sub>2</sub>OH or metal ion, identical and overlapping patterns of initial velocity were obtained (data not presented).

*Kinetics of Mg<sup>2+</sup> activation*—The saturation of *A.*

*niger* enzyme with  $Mg^{2+}$  at different fixed concentrations of ATP (termed  $Mg^{2+}$ -profiles) as well as the pattern of ATP saturation at different fixed concentrations of  $Mg^{2+}$  (termed ATP-profiles) was determined. It can be seen from Fig. 1A that all the  $Mg^{2+}$ -profiles were sigmoid and their sigmoidicity was dependent on the concentration of ATP present (increasing sigmoidicity with increasing fixed concentration of ATP). Also, there was no inhibition at higher concentrations of  $Mg^{2+}$ . Maximal activity was obtained when  $Mg^{2+}$  and ATP ratio was about 2:1. The marginal inhibition (5-10%) at the highest concentration of  $Mg^{2+}$  tried was not significant and was probably due to changes in the ionic strength.

There was no apparent sigmoidicity in the ascending limbs of ATP-profiles (Fig. 1B) but after the peak of activity was reached, increasing concentrations of ATP caused progressively larger inhibition of enzyme activity. The maximal velocity in each case was different and was dependent on the fixed concentration of  $Mg^{2+}$ . The peak positions were at  $Mg^{2+}$ : ATP ratio of approx. 2:1. When  $Mg^{2+}$  was present in excess (40 mM) over ATP (10 mM), the ATP-profile was hyperbolic. A  $K_m$  value of 1.5 mM was obtained for  $Mg^{2+}$ -ATP complex from a double-reciprocal plot.

The Dixon-plots for inhibition by ATP were drawn (Fig. 2A) using the data from the descending limbs of ATP-profiles (Fig. 1B). The plot shown in Fig. 2A is nonlinear (parabolic) indicating multiple interacting sites for ATP on the enzyme. The nonlinearity of the Dixon-plots precluded the determination of the  $K_i$  value for free ATP from these curves. Hence it was obtained from the isoveloccity replot of the data

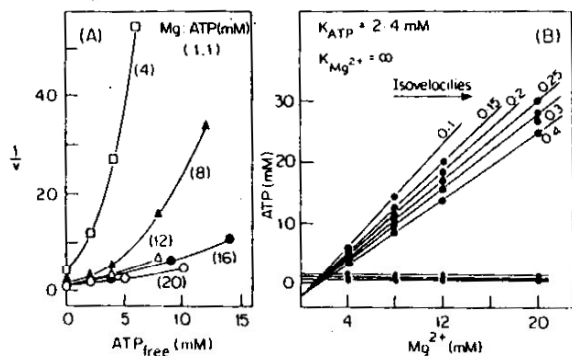


Fig. 2—Kinetics of inhibition of *A. niger*  $Mg^{2+}$ -dependent glutamine synthetase activity by ATP [(A), Dixon plot for ATP inhibition. Replot of data from the descending limbs of ATP saturation (Fig. 1B). The free ATP concentration was computed as follows:  $[ATP]_{free} = [ATP]_{total} - [Mg^{2+}]_{total}$  (eqn. 7) and the 1:1 complex of  $Mg$ .ATP was assumed to be the true substrate. (B), Isoveloccity replot of ATP profiles. The isoveloccity data from Fig. 1B (broken horizontal lines) were used and the two concentrations of ATP at each  $MgCl_2$  concentration were plotted as coordinate axes]

presented in Fig. 1B (broken horizontal lines). At each isoveloccity point, the two concentrations of ATP for each  $Mg^{2+}$  concentration were obtained by extrapolation. These two sets of extrapolated ATP concentrations were plotted against the corresponding concentration of  $Mg^{2+}$  according to London and Steck<sup>14</sup>. At low ATP concentrations ( $Mg^{2+}$  excess region), the isoveloccity replots (Fig. 2B) were linear and parallel to  $Mg^{2+}$ -axis. On the other hand, at higher ATP concentrations, a set of intersecting lines (Fig. 2B) was obtained and the point of intersection on the ATP axis gave a  $K_{ATP}$  value of 2.4 mM.

**Kinetics of  $Mn^{2+}$  activation**—The velocity profiles for  $Mn^{2+}$ -dependent synthetase activity were studied at its pH optimum of 5.5. The  $Mn^{2+}$ -profiles (Fig. 3A) were bell shaped with sigmoid ascending limbs. The position of the peak velocity was dependent upon the fixed concentration of ATP and maxima were reached

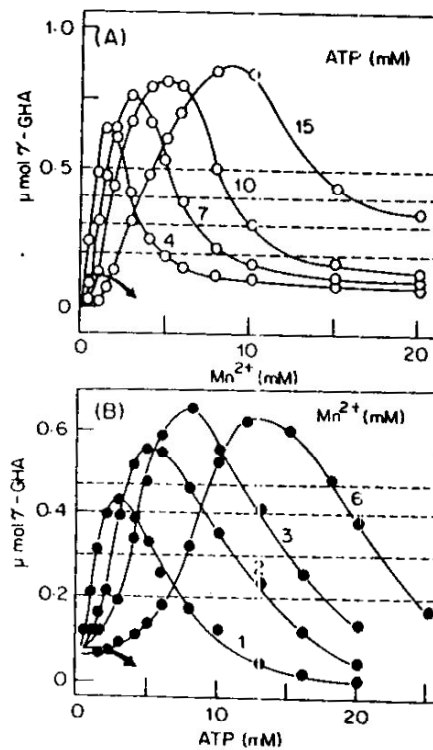


Fig. 3— $Mn^{2+}$  and ATP-saturations of *A. niger*  $Mn^{2+}$  dependent glutamine synthetase activity [(A),  $Mn^{2+}$ -profiles. The reaction mixture (0.5 ml) contained 100 mM imidazole hydrochloride buffer (pH 5.5), 50 mM  $NH_4OH$  and 100 mM L-glutamate.  $MnSO_4$  concentration was varied in the range 0-20 mM at 4, 7, 10 and 15 mM ATP. The reaction was started by the addition of enzyme (16  $\mu$ g). (B), ATP-profiles. The reaction mixtures were same as described above except that ATP concentrations were varied in the range 0-25 mM at 1, 2, 3 and 6 mM  $MnSO_4$ . Arrows indicate the shift of curves with increasing fixed concentrations of the ligand. Broken horizontal lines represent the isoveloccities used in the replots shown in Fig. 4]

at  $Mn^{2+}$ :ATP ratio of about 1:2. The sigmoidicity of the ascending limbs increased with increasing fixed concentration of ATP (arrow in Fig.3A). It is interesting to note that unlike  $Mg^{2+}$ -profiles (Fig. 1A), the  $Mn^{2+}$ -profiles showed a distinct inhibitory phase.

The ATP-profiles for the  $Mn^{2+}$ -supported synthetase assay are shown in Fig.3B. The velocity profiles were once again bell shaped with sigmoid ascending limbs. The sigmoidicity was more apparent at higher fixed concentrations of  $Mn^{2+}$  and the peak velocity occurred when  $Mn^{2+}$ :ATP ratio was about 1:2.

The constants  $K_{ATP}$ ,  $K_{Mn^{2+}}$  and  $K_{Mn^{2+} \cdot ATP}$  were obtained by isovelocitivity analysis<sup>14</sup> of the data. The two concentrations, of  $Mn^{2+}$  corresponding to a fixed concentration of ATP at each isovelocitivity point (broken horizontal lines in Fig.3A) from  $Mn^{2+}$ -profiles were plotted. In this replot, a family of lines, defined by the equation,

$$V[ATP]_{total} + v \cdot K_{ATP} - [v + (V-v) \frac{K_{ATP}}{K_{Mn^{2+} \cdot ATP}}] [Mn^{2+}]_{total} = 0 \quad \dots (3)$$

(where  $v$  is the isovelocitivity and  $V$  is the maximal

velocity) for the ATP excess region ( $[ATP] \gg [Mn^{2+}]$ ) intersect on ATP-axis to give  $K_{ATP}$  value of 1.2 mM (Fig. 4A). On the other hand at high  $Mn^{2+}$  concentration ( $Mn^{2+}$  excess region  $[Mn^{2+}] \gg [ATP]$ ), the curves follow the equation.

$$v[Mn^{2+}]_{total} + v \cdot K_{Mn^{2+}} - [v + (V-v) \frac{K_{Mn^{2+}}}{K_{Mn^{2+} \cdot ATP}}] [ATP]_{total} = 0 \quad \dots (4)$$

and intersect on the  $Mn^{2+}$  axis at a  $K_{Mn^{2+}}$  value of 0.7 mM. A similar analysis of ATP-profiles using points of equal velocity (broken horizontal lines in Fig.3B) gave  $K_{ATP}$  and  $K_{Mn^{2+}}$  values of 1.0 mM and 0.5 mM respectively (Fig.4B). The constants obtained for  $Mn^{2+}$  and ATP from ATP- and  $Mn^{2+}$ -profiles were similar and an average of the two values is presented (Table 2). The slopes of the asymptotically linear portions of the isovelocitivity replots (Fig.4A and B) in the  $Mn^{2+}$  excess region is given by,

$$\frac{d[Mn^{2+}]}{d[ATP]} = 1 - \frac{K_{Mn^{2+}}}{K_{Mn^{2+} \cdot ATP}} + V \frac{K_{Mn^{2+}}}{K_{Mn^{2+} \cdot ATP}} \cdot 1/v \dots (5)$$

Therefore these slopes when replotted against the

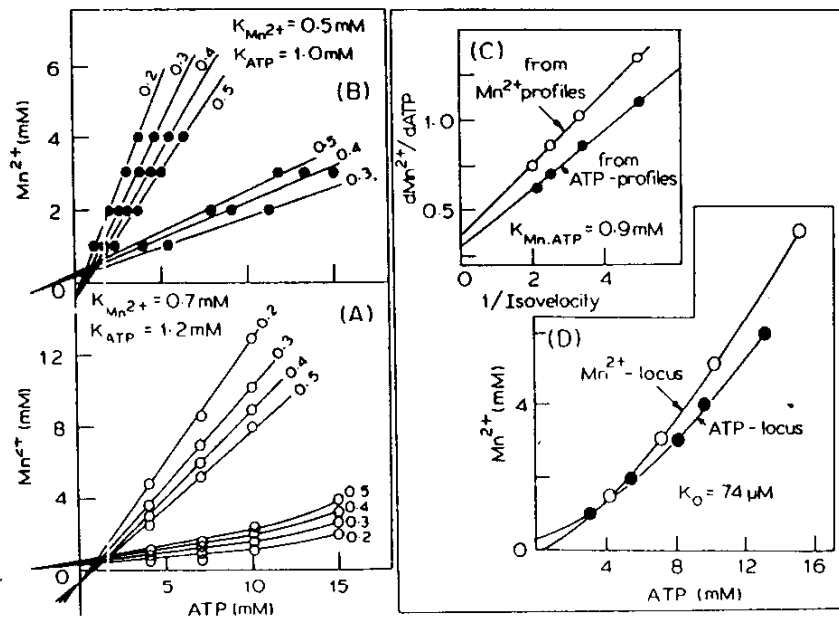


Fig. 4—Replots for the determination of  $K_{Mn^{2+}}$ ,  $K_{ATP}$ ,  $K_{Mn^{2+} \cdot ATP}$  and  $K_0$  for the  $Mn^{2+}$ -dependent synthetase reaction [(A). The plot of the two concentrations of  $Mn^{2+}$  corresponding to a fixed concentration of ATP at the isovelocities indicated by broken lines in Fig.3A. (B), a plot of the two concentrations of ATP corresponding to a fixed concentration of  $Mn^{2+}$  at the isovelocities indicated by broken lines in Fig.3B. (C), a plot of the slopes ( $d[Mn^{2+}]/d[ATP]$ ) of the asymptotically linear portion of the isovelocitivity replots in the  $Mn^{2+}$  excess region (Fig.4A and B) against the reciprocal of corresponding isovelocities from  $Mn^{2+}$ -profiles (O) and ATP-profiles (●). (D), locus of peak velocities. A plot of the concentration of  $Mn^{2+}$  and ATP at the peak velocity for each of the ATP-profiles (●) and  $Mn^{2+}$ -profiles (O)]

reciprocals of corresponding isovelocities gave a straight line (Fig.4C) and from the Y-axis intercept ( $= 1 - \frac{K_{Mn^{2+}}}{K_{Mn^{2+},ATP}}$ ), the value of  $K_{Mn^{2+},ATP}$  was calculated

to be 0.9 mM. This  $K_{Mn^{2+},ATP}$  value is an average of the values obtained from the analysis of  $Mn^{2+}$  excess region of ATP-profiles ( $=0.86$  mM) and  $Mn^{2+}$ -profiles ( $=0.95$  mM). Only data from  $Mn^{2+}$  excess region ( $[Mn^{2+}] > [ATP]$ ) were used as they were more accurate.

The concentrations of  $Mn^{2+}$  and ATP at the peak velocity for each of the ATP-profiles (Fig.3B) and  $Mn^{2+}$ -profiles (Fig.3A) were plotted as coordinate axes (called 'locus of the peak velocities'). Such an analysis of ATP-profiles (intercept on ATP-axis,  $K_o K_{ATP}$ , Fig. 4D) and  $Mn^{2+}$ -profiles (intercept on  $Mn^{2+}$  axis,  $K_o K_{Mn^{2+}}$ , Fig. 4D) gave  $K_o$  value of  $74 \mu M$  (Table 2) by substituting  $K_{ATP}$  and  $K_{Mn^{2+}}$ , independently determined in this study. A summary of the kinetic constants is given in Table 2.

Velocity profile at equimolar ratios of ATP and  $Mn^{2+}$  but at different concentrations was sigmoidal with half-maximal saturation at 18 mM (Fig.5).

**Determination of binding constants for  $Mg^{2+}$ -ATP complex and  $Mn^{2+}$  by their ability to protect against inactivation of the enzyme by phenylglyoxal and NEM—*A. niger* glutamine synthetase was completely inactivated by reaction with two moles of**

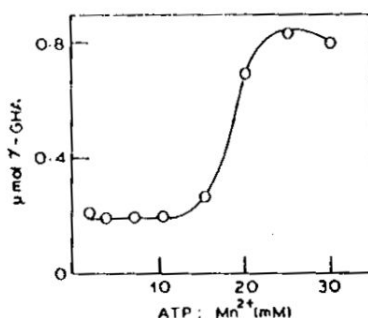


Fig. 5—Effect of varying ATP and  $Mn^{2+}$  concentration at equimolar ratio [The enzyme assays were performed in the same manner as described in the legend to Fig.3A except that the reaction mixtures contained different amounts of ATP and  $Mn^{2+}$  but in equimolar concentrations. Twelve  $\mu g$  of the enzyme was used per 0.5 ml of the assay mixture.]

phenylglyoxal or by one mole of NEM. The second order rate constants (at 28°C and pH 7.5) were determined to be  $3.8 M^{-1} min^{-1}$  and  $760 M^{-1} min^{-1}$ ; for phenylglyoxal and NEM respectively<sup>9</sup>. In order to evaluate the binding constant for  $Mg^{2+}$ -ATP complex, the inactivation of the enzyme by phenylglyoxal was carried out in the presence of increasing concentrations of this ligand. The protection by  $Mg^{2+}$ -ATP complex was reflected by decreased pseudo-first order rates of inactivation ( $k_{app}$  values, inactivation profiles and first order plots are not shown). A replot of this data shown in Fig.6 gave a  $K_{Mg^{2+},ATP}$  (dissociation constant for E. $Mg^{2+}$ -ATP complex) of 0.9 mM. A similar experiment for  $Mn^{2+}$ -ATP dependent synthetase activity (pH 5.5) was different from the pH for the inactivation (pH 7.5).

The  $K_{app}$  values for phenylglyoxal inactivation in the presence of increasing ATP:  $Mg^{2+}$  ratio followed a sigmoid pattern (Fig.7). Decreasing this ratio below 1:1 enhanced the protection as reflected by the decreased  $k_{app}$  values. On the other hand, when the ratio was higher, i.e. when there was a larger amount of free ATP in the mixture, the rate constants for inactivation were considerably larger. The effect of different ratios of ATP:  $Mg^{2+}$  on NEM inactivation of the *A. niger* enzyme was similar (Table 3) and protection was maximal around ATP:  $Mg^{2+}$  ratio of 1:1 to 1:2. Like in the case of phenylglyoxal inactivation, free ATP enhanced the rate of inactivation of the enzyme by NEM.

Free ATP also increased the rate of inactivation by phenylglyoxal in a concentration-dependent manner (Table 4), suggesting that E.ATP form of the enzyme was much more susceptible to this modification.

The enzyme was protected by low concentrations of  $Mn^{2+}$  ions against both (phenylglyoxal and NEM) inactivations in a concentration dependent manner.

Table 2—Kinetic and Dissociation Constants for the Interaction of Metal Ions, Nucleotide (ATP) and Metal Nucleotide Complexes with the *A. niger* Glutamine Synthetase

Ligand	Kinetic constant <sup>a</sup> (mM)	Dissociation constant <sup>b</sup> (mM)
<i>Mg<sup>2+</sup>-dependent synthetase activity</i>		
$Mg^{2+}$ -ATP complex	1.5	0.9
ATP	2.4	—
$Mg^{2+}$	x	—
<i>Mn<sup>2+</sup>-dependent synthetase activity</i>		
$Mn^{2+}$ -ATP complex	0.9	—
ATP	1.1	—
$Mn^{2+}$	0.6	0.052, 0.014 <sup>c</sup> $K_o = 0.074^d$

<sup>a</sup>Kinetic constants were obtained from saturation plots.

<sup>b</sup>Dissociation constants were obtained by measuring the protection afforded by the ligands against inactivation of the enzyme by phenylglyoxal.

<sup>c</sup>From protection experiments using NEM as the inactivating agent.

<sup>d</sup>Dissociation constant for the dissociation of  $Mn^{2+}$ -ATP complex into  $Mn^{2+}$  and ATP was calculated from replots of locus of peak velocities.

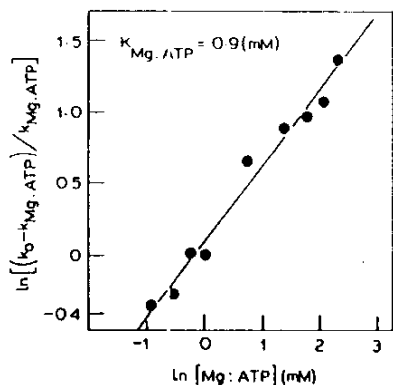


Fig. 6—The protection afforded to *A. niger* glutamine synthetase against phenylglyoxal inactivation by  $Mg^{2+}$ -ATP complex [The reaction mixtures containing the enzyme and different concentrations of  $Mg^{2+}$ :ATP (2:1 ratio and ATP varied between 0.4 to 10 mM) and 10 mM phenylglyoxal were incubated at pH 7.5, and at 28°C. Aliquots (50  $\mu$ l) were withdrawn at 5 min intervals and the enzyme activity remaining was estimated by the  $Mn^{2+}$ -dependent  $\gamma$ -glutamyl transferase assay. From the time course of inactivation (not shown), the first order plots were constructed for the determination of rate constants ( $k_{app}$ ) at the concentrations of  $Mg^{2+}$ -ATP used. A replot of this data as  $\ln[(k_0 - k_{Mg^{2+}-ATP})/k_{Mg^{2+}-ATP}]$  against  $\ln[Mg^{2+}:ATP]$  was used to evaluate the dissociation constant for the enzyme and  $Mg^{2+}$ -ATP complex]

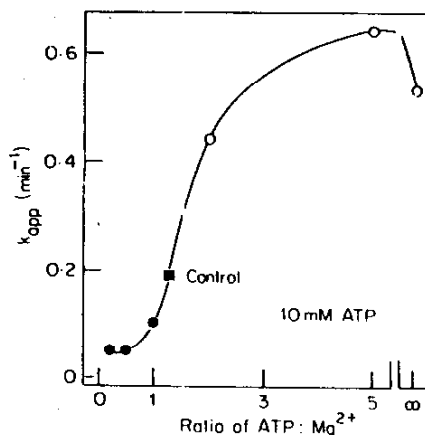


Fig. 7—Effect of different ratios of ATP: $Mg^{2+}$  on the  $k_{app}$  value for the inactivation of the enzyme by 10 mM phenylglyoxal. The inactivations were carried out in the same manner as described in Fig. 6, and  $k_{app}$  values were calculated from pseudo-first order plots. ATP was used at 10 mM concentration with different concentrations of  $MgCl_2$ . (■). Control—10 mM phenylglyoxal alone; (●). protection; (○) enhanced inactivation]

From replots of  $k_{app}$  values for the phenylglyoxal inactivation at different  $Mn^{2+}$  concentrations and from similar experiments carried out with NEM,  $K_{Mn^{2+}}$  values of 52  $\mu$ M and 14  $\mu$ M (Fig. 8A & B) were obtained. The binding constants obtained from protection experiments are also listed in Table 2.

Table 3—Effect of Different Concentrations of ATP and  $MgCl_2$  on the Inactivation of the Enzyme by NEM\*

ATP (mM)	$Mg^{2+}$ (mM)	$k_{app}$ ( $min^{-1}$ )
—	—	0.136
10	5	0.118
10	10	0.018
10	20	0.016
10	—	0.262

\*Inactivation mixtures contained 50 mM imidazolehydrochloride buffer (pH 7.5), 0.4 mM NEM and enzyme (55  $\mu$ g/500  $\mu$ l) which was passed through a column of Sephadex G-25 to remove 2-mercaptoethanol, (For details, see Experimental Procedures) and  $MgCl_2$  and ATP at concentrations indicated. Aliquots (50  $\mu$ l) were withdrawn at 5 min intervals and the amount of active enzyme remaining was measured by  $Mn^{2+}$ -dependent  $\gamma$ -glutamyltransferase assay.  $k_{app}$  values were computed from the pseudo-first order plots

Table 4—Effect of ATP on the Inactivation of *A. niger* Glutamine Synthetase by Phenylglyoxal\*

ATP (mM)	$k_{app}$ ( $min^{-1}$ )
0.0	0.029
0.1	0.041
0.5	0.057
0.7	0.064
1.0	0.083
2.0	0.162
4.0	0.217
6.0	0.281
8.0	0.351
10.0	0.393

\*The inactivation of the enzyme by 4 mM phenylglyoxal was carried out at 28°C in 50 mM imidazole hydrochloride buffer (pH 7.5) and in the presence of concentrations of ATP shown in the table. Aliquots (50  $\mu$ l) were withdrawn at 5 min intervals and the enzyme activity remaining was measured by  $Mn^{2+}$ -dependent  $\gamma$ -glutamyl transferase assay.  $k_{app}$  values were calculated from the pseudo-first order plots.

## Discussion

Glutamine synthetase from *A. niger* specifically required either  $Mn^{2+}$  or  $Mg^{2+}$ -ATP complex as substrate<sup>9</sup>. Although other divalent metal ions, e.g.  $Ca^{2+}$ ,  $Zn^{2+}$  and  $Co^{2+}$ , ATP complexes were not substrates for the biosynthetic reaction, their importance and possibly physiologically significant role in the *in vivo* regulation of this enzyme activity is indicated by the results presented in Table 1. Inhibitory effect of these divalent metal ions (Table 1) as well as the inhibition by  $Mn^{2+}$  of the  $Mg^{2+}$ -supported synthetase activity suggested the probable existence of an additional metal ion binding site on the enzyme for  $Mn^{2+}$ .

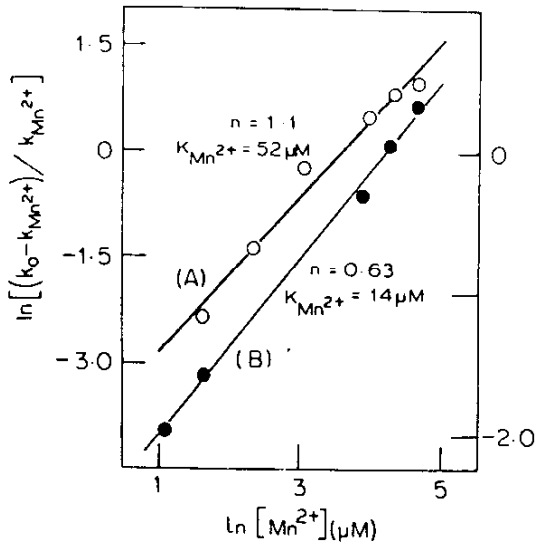
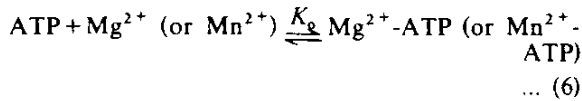


Fig. 8—Protection of *A. niger* glutamine synthetase against (A) phenylglyoxal and (B) NEM inactivation by  $Mn^{2+}$  ions [The inactivations were carried out as described in the legend for Fig. 6 using 10 mM phenylglyoxal or 0.4 mM NEM but in the presence of 0–100  $\mu M$   $MnSO_4$ . From the  $k_{app}$  values obtained for both the inactivations at each  $Mn^{2+}$  concentration,  $\ln[(k_0 - k_{Mn^{2+}})/k_{Mn^{2+}}]$  versus  $\ln[Mn^{2+}]$  was plotted. The enzyme activity was monitored by  $Mn^{2+}$ -dependent  $\gamma$ -glutamyl transferase assay. The enzyme was passed through Sephadex G-25 column to remove 2-mercaptoethanol prior to measuring the inactivation by NEM.]

The effect of GTP on the *A. niger* glutamine synthetase activity was probably due to its metal complexing property and not due to feed-back inhibition as an end product of glutamine metabolism. The binding constant for ATP with  $Mg^{2+}$  or  $Mn^{2+}$  is comparable to that of GTP and hence it could shift the following equilibrium



to the left resulting in a decrease in the effective concentration of the true substrate (metal-ATP complex) as well as an increase in the concentration of free ATP in the mixture. A combined effect of these would be a marked decrease in the velocity. This conclusion is supported by the observations that  $Mg^{2+}$  or  $Mn^{2+}$ -GTP complexes do not act as substrates: GTP is able to overcome inhibition caused by excess  $Mn^{2+}$  and GTP inhibition can be overcome by increasing the concentration of divalent metal ion ( $Mg^{2+}$  or  $Mn^{2+}$ ). Further support for this conclusion was the observation that a well known metal chelator, EDTA, gave similar results, although a more pronounced inhibition was observed (Table I).

The results obtained on the effects of  $Mg^{2+}$  and

$Mn^{2+}$  on *A. niger* glutamine synthetase were analyzed using the criteria suggested by London and Steck<sup>14</sup> for metal activation namely: (a) nature of the ascending limbs of the velocity profiles; (b) relative position of the profiles obtained at higher fixed concentrations of ATP or metal ion; (c) the presence and position of peak velocity; (d) sigmodicity of the velocity profile with varied concentration but at equimolar ratio of metal ion and ATP; and (e) the velocity when metal ion or ATP was present in comparative excess.

Based on the kinetic experiments (Fig. 1-5) and the protection afforded by  $Mn^{2+}$  against inactivation of the enzyme by phenylglyoxal and NEM (Figs 6 & 8) as well as our earlier observations<sup>8,9</sup>, the general model proposed by London & Steck can be used to explain the interaction of  $Mn^{2+}$ ,  $Mg^{2+}$  and ATP with *A. niger* glutamine synthetase (Fig. 9). The forward triangle of the bottom face of the cube represents the equilibria for  $Mg^{2+}$ -supported activity and the entire bottom face represents the equilibria for the  $Mn^{2+}$ -dependent activity of *A. niger* glutamine synthetase. It should be emphasized at the outset that this mechanism does not make any assumptions regarding the order of binding of substrates or release of products. The observation with glutamine synthetase from different sources<sup>17</sup> suggests that a random kinetic mechanism may be operative. E (therefore represents free enzyme or enzyme complexed with either  $NH_2OH$ , L-glutamate or both) binds  $Mg^{2+}$ -ATP complex with a kinetic constant  $K_{Mg^{2+}\text{-ATP}}$  (1.5 mM) to yield a productive enzyme substrate complex which turns over to yield free enzyme and products. E also binds free ATP ( $K_{ATP} = 2.4$  mM) but not free  $Mg^{2+}$  in a kinetically significant manner as indicated by the absence of inhibition at excess  $Mg^{2+}$  and by the failure of this metal ion to afford protection against inactivation. As free ATP and  $Mg^{2+}$ -ATP complex compete for the same enzyme form, ATP is a competitive inhibitor with respect to  $Mg^{2+}$ -ATP.

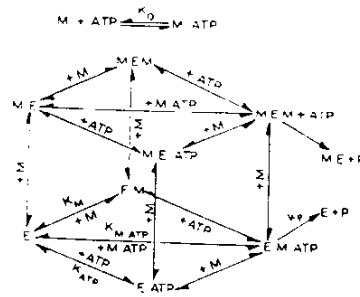


Fig. 9—Equilibria for the interaction of metal ion M ( $Mg^{2+}$  or  $Mn^{2+}$ ) and ATP with *A. niger* glutamine synthetase based on the general model of London and Steck<sup>14</sup> for metal ion, nucleotide and enzyme interactions



Similar values of Michaelis constant for  $Mg^{2+}$ -ATP (1.5 mM) and the dissociation constant obtained from protection experiments (0.9 mM, Fig. 6) suggested that binding at the active site was probably being monitored in both the cases. The sigmoid pattern of enhancement of enzyme activity when ATP- $Mg^{2+}$  concentration was varied (Fig. 1A) and protection against phenylglyoxal (Fig. 7) and NEM (Table 3) inactivation are in support of the above suggestion.

Further support for the kinetic experiment suggesting that free ATP was binding to the enzyme was the observation that free ATP enhanced the rate of inactivation by phenylglyoxal (Table 4) or NEM (Table 3). Using modification by NEM it was demonstrated that mammalian glutamine synthetase was binding ATP and Mg-ATP complex at different sites<sup>18</sup>.

In the case of  $Mn^{2+}$ -dependent glutamine synthetase activity, E reacts with  $Mn^{2+}$ -ATP complex with a kinetic constant  $K_{Mn^{2+}-ATP}$  (0.9 mM) to form E. $Mn^{2+}$ -ATP complex, which decomposes to form products and regenerates E. In addition, E also binds to  $Mn^{2+}$  or ATP separately with constants  $K_{Mn^{2+}}$  (0.6 mM) and  $K_{ATP}$  (1.1 mM) respectively. ATP reacts with free metal ion ( $Mn^{2+}$ ) with a dissociation constant  $K_o$  to yield the  $Mn^{2+}$ -ATP complex, which is the true substrate for the reaction. Hence it is evident that the velocity of  $Mn^{2+}$ -dependent synthetase reaction is dependent on the concentrations of  $Mn^{2+}$ -ATP and  $Mn^{2+}$ -ATP complex along with the four constants, namely,  $K_{Mn^{2+}}$ ,  $K_{ATP}$ ,  $K_{Mn^{2+}-ATP}$  and  $K_o$  (Table 2). The inhibition by excess metal ion is characteristic of the  $Mn^{2+}$ -supported biosynthetic activity when compared to the  $Mg^{2+}$ -dependent reaction of *A. niger* glutamine synthetase. Additional evidence in support of  $Mn^{2+}$  interaction with the enzyme was the observation that GTP, which is not a substrate for the enzyme, relieved the inhibition caused by excess  $Mn^{2+}$  (Table 1) by complexing with it and making it unavailable for interaction.

Independent evidence for the interaction of  $Mn^{2+}$  with the enzyme (in addition to  $Mn^{2+}$ -ATP complex functioning as a substrate) was obtained by monitoring the protection afforded by low concentrations of  $Mn^{2+}$  against inactivation of the enzyme by NEM and phenylglyoxal (Fig. 8). This  $Mn^{2+}$  protection and 'n' value of about one ( $K_{Mn^{2+}} = 52 \mu M$  and  $n = 1.1$ , Fig. 8A and  $K_{Mn^{2+}} = 14 \mu M$  and  $n = 0.63$ , Fig. 8B) suggested the presence of at least one high affinity,  $Mn^{2+}$ -binding site on the enzyme. The kinetic constant for  $Mn^{2+}$  (0.6 mM) was an order of magnitude higher than the binding constant obtained from protection experiments, indicating that there are probably more than one class of  $Mn^{2+}$  binding sites on the enzyme. The presence of high affinity site for  $Mn^{2+}$  was also

suggested by the inhibition of  $Mg^{2+}$ -dependent synthetase activity by low concentrations of  $Mn^{2+}$ . A number of studies have shown that *Escherichia coli* glutamine synthetase has one tight binding, one intermediate binding and up to four weak metal ion binding sites per catalytic subunit<sup>19-23</sup>. Both tight binding ( $n_1$ ) and intermediate binding ( $n_2$ ) sites have been postulated to have a role in the catalytic activity of *E. coli* glutamine synthetase. However, in the case of *A. niger* enzyme, the  $n_1$  sites represent the high affinity binding of free metal ion ( $Mn^{2+}$ ) and  $n_2$ , the low affinity site, where Mn-ATP complex binds as one of the substrates. This mechanism is represented by the top face of the equilibrium cube (Fig. 9). A recent report of a parallel study has led to the conclusion that glutamine synthetase from ovine brain may be a manganese (II) enzyme<sup>3</sup>. This enzyme, unlike glutamine synthetase from *A. niger*, shows high affinity kinetic interaction for both  $Mn^{2+}$  as well as  $Mg^{2+}$ , whereas the latter does not contain a kinetically meaningful high affinity site for  $Mg^{2+}$  ions.

The  $K_m$  values for  $Mn^{2+}$ -ATP and  $Mg^{2+}$ -ATP (Table 2) agree well with a recent estimate<sup>24</sup> of the intracellular concentration of ATP (1 mM) in *A. niger* in view of the high affinity (site) for  $Mn^{2+}$  ( $n_1$  site) and the availability of sufficient amounts of  $Mn^{2+}$  within the *A. niger* cells<sup>25</sup>, it could be postulated that *A. niger* enzyme occurs as a  $Mn^{2+}$ -protein. It has been suggested that  $Mn^{2+}$  ions can act as intracellular regulators<sup>26,27</sup>. The results presented here clearly indicate that glutamine synthetase could be a locus for regulation by  $Mn^{2+}$  ions.

## References

1. Stadtman E R (1973) in *The Enzymes of Glutamine Metabolism* (Prusiner S & Stadtman E R, eds), pp 1-6, Academic Press, New York.
2. Stadtman E R & Ginsburg A (1974) *The Enzymes*, **10**, 755-807.
3. Wedler F C, Denman R B & Roby W G (1982) *Biochemistry*, **21**, 6389-6396.
4. Ip S M, Rowell P & Stewart W D P (1983) *Biochem Biophys Res Commun*, **114**, 206-213.
5. Kubicek C P & Rohr M (1977) *European J Appl Microbiol*, **4**, 167-175.
6. Habison H, Kubicek C P & Rohr M (1979) *FEMS Microbiol Lett*, **5**, 39-42.
7. Kubicek C P, Hampel W & Rohr M (1979) *Arch Microbiol*, **123**, 73-79.
8. Punekar N S (1983) *Regulation of Glutamine Synthetase and its Role in Citric Acid Fermentation by Aspergillus niger*, Ph D Thesis, Indian Institute of Science, Bangalore.
9. Punekar N S, Vaidyanathan C S & Appaji Rao N (1984) *J Biosci*, **6**, 17-35.
10. Rowe W S, Ronzio R A, Wellner V P & Meister A (1970) *Methods Enzymol*, **17A**, 900-910.
11. Lowry O H, Rosebrough N J, Farr A L & Randall R J (1951) *J Biol Chem*, **193**, 265-275.
12. Nelson C A, Hummel J P, Swenson C A & Friedman L (1962) *J Biol Chem*, **237**, 1575-1580.

- 13 Carter J R, Fox C F & Kennedy E P (1968) *Proc Natl Acad Sci USA*, **60**, 725-730.
- 14 London W P & Steck I L (1969) *Biochemistry*, **8**, 1767-1779.
- 15 Tu A T & Heller M J (1974) *Metal Ions in Biological Systems* (H Sigel, ed.), Vol. I, pp 1-49.
- 16 Kingdon H S, Hubbard J S & Stadtman E R (1968) *Biochemistry*, **7**, 2136-2152.
- 17 Meck T D & Villafrance J J (1980) *Biochemistry*, **19**, 5513-5519.
- 18 Jaenick L & Berson W (1977) *Hoppe-Seyler's Z. Physiol Chem.*, **358**, 883-889.
- 19 Hubbard J S & Stadtman E R (1967) *J Bacteriol.*, **94**, 1007-1015.
- 20 Stadtman E R, Shapiro B M, Ginsburg A, Kingdon H S & Denton M D (1969) *Brookhaven Symp Biol.*, **21**, 378-396.
- 21 Hunt J B, Smyrniotis P Z, Ginsburg A & Stadtman E R (1975) *Arch Biochem Biophys.*, **166**, 102-124.
- 22 Hunt J B & Ginsburg A (1980) *J Biol Chem.*, **255**, 590-594.
- 23 Balakrishnan M S & Villafrance J J (1979) *Biochemistry*, **18**, 1546-1551.
- 24 Kubicek C P & Rohr M (1980) *Biochim Biophys Acta*, **615**, 449-457.
- 25 Bowes I & Matthey M (1979) *FEMS Microbiol Lett.*, **6**, 219-222.
- 26 Williams R J P (1982) *FEBS Lett.*, **140**, 3-10.
- 27 Schramm V L (1982) *Trends Biochem Sci.*, **7**, 369-371.